AD_____

Award Number: W81XWH-04-1-0590

TITLE: Constrained Adaptive Beamforming for Improved Contrast in Breast Ultrasound

PRINCIPAL INVESTIGATOR: William F. Walker, Ph.D.

CONTRACTING ORGANIZATION: University of Virginia
Charlottesville, VA 22904

REPORT DATE: June 2005

20060223 031

TYPE OF REPORT: Annual

PREPARED FOR: U.S. Army Medical Research and Materiel Command
Fort Detrick, Maryland 21702-5012

DISTRIBUTION STATEMENT: Approved for Public Release;
Distribution Unlimited

The views, opinions and/or findings contained in this report are those of the author(s) and should not be construed as an official Department of the Army position, policy or decision unless so designated by other documentation.

REPORT DOCUMENTATION PAGE

Form Approved
OMB No. 0704-0188

Public reporting burden for this collection of information is estimated to average 1 hour per response, including the time for reviewing instructions, searching existing data sources, gathering and maintaining the data needed, and completing and reviewing this collection of information. Send comments regarding this burden estimate or any other aspect of this collection of information, including suggestions for reducing this burden to Department of Defense, Washington Headquarters Services, Directorate for Information Operations and Reports (0704-0188), 1215 Jefferson Davis Highway, Suite 1204, Arlington, VA 22202-4302. Respondents should be aware that notwithstanding any other provision of law, no person shall be subject to any penalty for failing to comply with a collection of information if it does not display a currently valid OMB control number. **PLEASE DO NOT RETURN YOUR FORM TO THE ABOVE ADDRESS.**

1. REPORT DATE *(DD-MM-YYYY)*
01-06-2005

2. REPORT TYPE
Annual

3. DATES COVERED *(From - To)*
1 Jun 04 – 31 May 05

4. TITLE AND SUBTITLE
Constrained Adaptive Beamforming for Improved Contrast in Breast Ultrasound

5a. CONTRACT NUMBER

5b. GRANT NUMBER
W81XWH-04-1-0590

5c. PROGRAM ELEMENT NUMBER

5d. PROJECT NUMBER

5e. TASK NUMBER

5f. WORK UNIT NUMBER

6. AUTHOR(S)
William F. Walker, Ph.D.

E-Mail: WFW5H@VIRGINIA.EDU

7. PERFORMING ORGANIZATION NAME(S) AND ADDRESS(ES)

University of Virginia
Charlottesville, VA 22904

8. PERFORMING ORGANIZATION REPORT NUMBER

9. SPONSORING / MONITORING AGENCY NAME(S) AND ADDRESS(ES)
U.S. Army Medical Research and Materiel Command
Fort Detrick, Maryland 21702-5012

10. SPONSOR/MONITOR'S ACRONYM(S)

11. SPONSOR/MONITOR'S REPORT NUMBER(S)

12. DISTRIBUTION / AVAILABILITY STATEMENT
Approved for Public Release; Distribution Unlimited

13. SUPPLEMENTARY NOTES

14. ABSTRACT

Abstract is on following page.

15. SUBJECT TERMS
Imaging, Ultrasound, Diagnosis, Non-Invasive

16. SECURITY CLASSIFICATION OF:			17. LIMITATION OF ABSTRACT	18. NUMBER OF PAGES	19a. NAME OF RESPONSIBLE PERSON
a. REPORT	b. ABSTRACT	c. THIS PAGE			USAMRMC
U	U	U	UU	31	19b. TELEPHONE NUMBER *(include area code)*

ABSTRACT

Ultrasonic imaging plays an important role as an adjunct to mammography, with an emerging role in breast cancer screening. Ultrasound's real-time nature, lack of ionizing radiation, and relative comfort for the patient make it an attractive imaging choice. Unfortunately, ultrasound image quality is often limited.

We hypothesize that bright scatterers seriously degrade ultrasound images by introducing image clutter. In the breast bright off-axis echoes may originate from Cooper's ligaments, structured glandular tissue, calcification, fat-soft tissue interfaces, or other structures.

While we initially proposed using a variant of the Frost Adaptive Beamformer to reduce clutter, we have since discovered that this technique is non-optimal for our application. Extensive literature reviews have led us to utilize a recently proposed method, Spatial Processing Optimized and Constrained (SPOC). In initial simulations this method not only dramatically reduces image clutter, but also yields super-resolution. We are actively refining this method while developing the experimental tools needed for in vivo testing.

Table of Contents

Cover.....

SF 298.....

Table of Contents.....3

Introduction.....4

Body.....6

- CAB Progress.....6
- Review of the Adaptive Beamforming Literature.....7
- SPOC Progress.....10
- Simulation Tool Development.....13
- Experimental Platform Development.....14

Key Research Accomplishments.....15

Reportable Outcomes.....16

Conclusions.....17

References.....18

Appendices.....19

Introduction:

Ultrasonic imaging currently plays an important role as an adjunct to mammography [1, 2]. Ultrasound's real-time nature, lack of ionizing radiation, and relative comfort for the patient make it an attractive choice for applications which include the differentiation of fluid filled cysts and solid masses, differentiation of benign and malignant lesions, and guidance of needle and core biopsy procedures. Recent studies have even shown the potential of ultrasound as a screening tool, especially for pre-menopausal women whose radio-dense breast tissue seriously limits x-ray mammography [3]. In both differential diagnosis and screening applications however, ultrasound image quality is limited, with high levels of background clutter representing a significant problem in many patients.

While the cause of high background clutter and poor breast image quality has not been determined with certainty, it is widely held that acoustic velocity inhomogeneities in breast tissue cause defocusing of the acoustic beam. This distortion manifests itself through mainlobe broadening and increasing sidelobe levels. Numerous researchers, including the Principal Investigator, have suggested that this problem, known as phase aberration, might be corrected through the application of compensating time delays [4-6], a combination of delay and amplitude corrections [7], or other more complex techniques [8-10]. While proposed phase aberration correction methods have been shown to have great potential in *ex vivo* or other non real-time environments, there has been limited evidence of significant clinical image improvement. The development of a real-time phase aberration correction system at the GE Global Research Center has shown that real-time phase correction is possible, however *in vivo* results using 1.5-D arrays show contrast improvements of only about 3 dB in the abdomen [11, 12]. This unimpressive outcome may result from imperfect algorithm optimization, or perhaps a lower level of *in vivo* phase aberration than previously suspected. This latter hypothesis is supported by recent phase aberration measurements performed at Duke University which indicate *in vivo* phase aberrations of only ~25ns RMS (Root Mean Squared) with a 3.5 mm FWHM (Full Width at Half Maximum) [13]. The limited improvements of real-time phase correction, coupled with low measured aberrations, suggest that phase aberration may not represent the major source of breast image degradation.

If phase aberration is not the primary factor limiting breast image quality, then what is? We hypothesize that localized bright scatterers seriously degrade ultrasound images by introducing broad image clutter. Figure 1 shows single channel Radio Frequency (RF) echo data obtained from calcifications in the thyroid of a human subject at Duke University. A focused transmit beam was used and RF data was acquired from each element in a 1.5-D array consisting of approximately 1000 elements. Figure 1 shows data from one row of this array after application of geometrically determined focal delays. At least three clear waveforms are visible in this data set, with each probably resulting from a single calcification. Although summation across channels to form an RF image line would amplify the echo coming from directly in front of the array, it would not entirely eliminate the two other visible targets. These non-focal targets would appear in this image line as clutter, reducing image contrast. In addition to the three dominant calcification waveforms, the data set also includes echoes from background speckle. These background echoes also include discernable off-axis scatterers that undoubtedly generate further clutter in the image. Note that the thyroid data presented in figure 1 is similar in appearance to breast data obtained at Duke. In the breast bright off-axis echoes may originate from Cooper's ligaments, highly structured glandular tissue, calcification, fat-soft tissue interfaces, or other tissue structures.

The presence of bright off-axis scatterers and the image degradation that they cause is not surprising. It is well known that the acoustic reflectivity of targets within the body covers many orders of magnitude. It is precisely for this reason that manufacturers employ aggressive apodization to reduce sidelobe levels in diagnostic ultrasound. It has also been argued that harmonic imaging is effective at improving image quality because it further reduces sidelobe levels and therefore reduces the spatial spread of bright targets. The detrimental impact of bright scatterers on ultrasound image quality is recognized in experimental data, physical intuition, and years of experience in ultrasound system design.

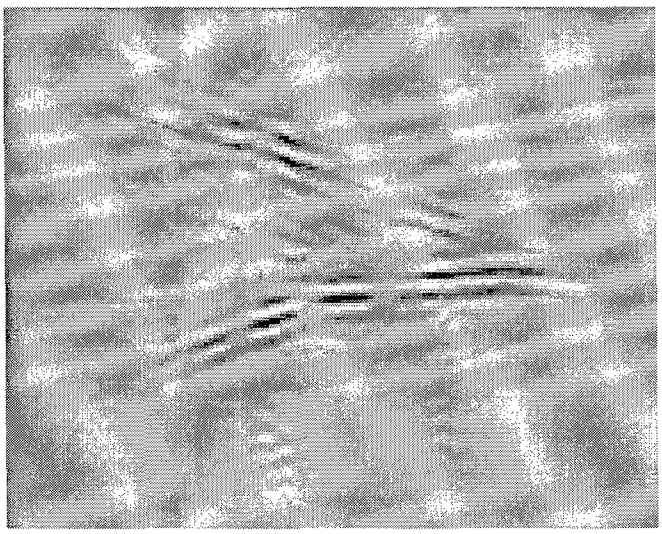

Figure 1: Single channel data obtained *in vivo* from a human thyroid. At least three bright scatterers (likely microcalcifications) are visible. While one target lies near the focus, the other two are off-axis and will contribute clutter to this image line. Off-axis targets are also visible within the speckle generating background echoes. (Data courtesy Gregg Trahey, Duke University.)

The impact of a few bright targets in an otherwise dim image has been well studied in both RADAR and SONAR. In SONAR the detection of an intentionally stealthy submarine among many noisy ships requires separating out a signal that is orders of magnitude below the signals from other nearby targets. A broad variety of adaptive beamforming algorithms have been developed for this scenario. It is the goal of this research project to evaluate the potential applicability of these methods in medical ultrasound.

Body:

CAB Progress:

In our original proposal we described a research plan to explore the potential of one particularly elegant and well studied method for adaptive beamforming. This technique, developed by Frost in the early 70s, represents the beamforming process using a linear algebra formulation. A set of beamformer weights, corresponding to an individual FIR filter for each element of the array, is determined adaptively from the data acquired by the sensor array. The weights are determined so as to minimize the energy in the beamsum signal, subject to the constraint that the beamformer must exhibit a given impulse response for signals received from the array look direction. Over decades of analysis, the Frost Adaptive Beamformer (FAB) has proven to be a valuable tool for identifying dim targets within clutter backgrounds.

In work performed prior to the initiation of this grant we built upon FAB and modified it to account for the unique characteristics of medical ultrasound. The resultant algorithm, referred to as the Constrained Adaptive Beamformer (CAB), works in transmit-receive systems, can be applied to near-field data, and can handle the broad bandwidths and limited stationarity of ultrasound data [14, 15]. As our initial proposal indicated, the CAB showed great potential with both simulation and experimental ultrasound data.

Unfortunately CAB presented significant difficulties. First, because our implementation of the CAB required the inversion of large matrices for each pixel in the output image, the computational cost of implementing CAB was enormous. Computation of modest images only a few millimeters on a side took a day or more on a high-end PC. While irritating, this limitation was not considered fundamental. More serious was the problem of target dependency that we found as we applied CAB to various data sets. When applied to point target data we found that straight-forward implementation of the algorithm termed Single-Iteration CAB (SI-CAB) yielded excellent results; the main-lobe was narrowed and sidelobes were reduced, improving both spatial resolution and image contrast. When we applied the same algorithm to data from a point target embedded within a speckle target however the results were much more complicated. While the center of the point target was better focused, strange behavior was exhibited in the "tails" or side-lobes of the point response. In these areas the algorithm not only eliminated the clutter contribution of the bright target, but it also eliminated the background speckle signal. Thus the output image was basically black in the tail regions of point target, regardless of what sort of target was actually present. This was clearly an unsatisfactory result. In an attempt to compensate for this problem a previous student of the Principal Investigator (Jake Mann) developed an alternate version of the algorithm that he called Multi-Iteration CAB or MI-CAB. This algorithm repeatedly performed the SI-CAB algorithm on windows of data with partial overlap. It then averaged output results in areas of overlap. Although this approach eliminated some of the artifacts present in speckle regions it also showed much worse performance than SI-CAB for point targets. Thus we were left with the highly unsatisfactory situation of requiring different algorithms for different target types.

Upon initiation of this grant I decided that it was critical that we not only understand CAB more thoroughly and fundamentally than we had before, but that we also explore the broad array of adaptive beamforming methods that had been developed since Frost's seminal work in 1972. These two goals were far from independent; the insights gained in the literature review gave us many new insights into the potential and limitations of CAB.

In our review of the literature we came to realize more deeply that the FAB was designed for problems that were fundamentally different than that we face in ultrasound imaging. We were reminded that the FAB was designed to address situations where the targets were in the far-field of the imaging array and where the acoustic environment was effectively narrowband. These assumptions we had been aware of and had addressed carefully in the design of CAB. What we had been less clear about was the assumption made by FAB that there would be multiple, statistically independent, signal realizations available from any given field of targets. In medical ultrasound this assumption is completely wrong. We can only get one realization of the signals from any particular target arrangement. (This is not strictly true if compounding is applied, but in normal imaging this is a

fair assessment.) This difference proves to be huge and is the main reason that we found such poor behavior when applying CAB to speckle targets. While compounding could theoretically be used to get multiple independent looks at the target, a careful review of the literature indicated that practical compounding schemes could never yield enough independent looks to provide statistically robust performance. Thus a careful literature review followed by a series of well designed computer simulations showed us that CAB was a fundamentally flawed algorithm for medical ultrasound imaging. Clearly we would need to identify another algorithmic foundation for this research effort.

Review of the Adaptive Beamforming Literature:

Our review of the adaptive beamforming literature covered dozens of papers and for many of these we followed up by coding the described algorithms in MATLAB and testing their performance on simulation ultrasound data. In the process of reviewing this area we found it particularly helpful to categorize algorithms depending upon their assumptions and limitations. There were obvious differences between algorithms that were developed for near-field application and those intended for far-field implementation. Likewise, algorithms intended for narrow-band signals could be readily differentiated from those intended for broad-band signals. For both of these differentiators we found, as we had with the development of CAB, that it was often (although not always) straightforward to identify algorithm modifications that would move them from one domain to another. A more fundamental difference, that was much less clear at the beginning of our work, was the importance of the number of available realizations of the data. Specifically, some algorithms assumed that data from the targets could be acquired repeatedly with each acquisition offering a new statistical realization of the system. Other algorithms assumed that only one look at the data was available. This difference proves to be critical in our problem.

To summarize, the problem of adaptive beamforming in breast imaging can generally be stated as utilizing broad-band signals, operating in the near-field of the transducer arrays, and operating on only one look at the target.

In the following sections we summarize our findings in the adaptive beamforming literature and classify algorithms in terms of their assumptions and potential for our problem.

STATISTICAL BEAMFORMERS

The following beamformers make use of the second order statistic of the data in order to determine filter weights for the rejection of off-axis signals. They have been well characterized and some have been known for decades.

> **CAPON BEAMFORMER** (also know as the Minimum Variance Distortionless Response, or MVDR, beamformer)
> This algorithm solves for a weight vector that minimizes the energy of the beamformer's output given a linear constraint. The sum of the weights is equal to some number g (generally, g=1).
> The Capon BF requires narrowband signals.
> The main drawback of this algorithm is that it requires knowledge of the second order statistics of the data (i.e., autocorrelation matrix). The autocorrelation matrix cannot be reliably determined without acquiring many statistically independent looks at the target. This is not possible in medical ultrasound, because even compounding does not yield enough independent looks to produce a useful image.
>
> J. Capon, "High resolution frequency-wavenumber spectrum analysis," *Proc. IEEE*, vol. 57, pp. 1408-1418, 1969.

FROST BEAMFORMER

Also in this case, a weight vector is chosen to minimize the output energy given a linear constraint on the weights. The main difference with the Capon BF is that this algorithm uses K taps in time, therefore allowing the use of broadband signals.

Again, the autocorrelation matrix of the data is required. Furthermore, significant problems occur if the signal of interest and noise (off-axis signal) are correlated (i.e., they have the same spectral response). This is a common occurrence in medical ultrasound.

O. L. Frost III, "An Algorithm for Linearly Constrained Adaptive Array Processing," *Proc. IEEE*, vol. 60, no. 8, pp. 926-935, 1972.

GENERALIZED SIDELOBE CANCELLOR (Griffith's formulation)

Equivalent to the Frost algorithm in its formulation and assumptions. The main advantage of the GSC is that it transforms the minimization from constrained to unconstrained, therefore increasing the degree of freedoms of the beamformer. This is accomplished using a subtractive process on the array elements. The GSC has many of the same limitations as the Frost BF, but is somewhat easier to implement.

L. J. Griffith and C. W. Jim, "An Alternative Approach to Linearly Constrained Adaptive Beamforming," *IEEE Trans. Antennas Propagat.*, vol. AP-30, no. 1, pp. 27-34, 1982.

DUVALL BEAMFORMER

Equivalent to the Frost beamformer in its formulation and assumptions. This algorithm, however, is designed to get around the problem of correlated signal and noise. This is critical for medical ultrasound, where clutter usually results from reflection of the same pulse as that used to image the target. The Duvall BF uses two BFs; the first one is a slave BF, whereas the second is connected to the array elements through a subtractive process. The weights calculated in the latter BF are then copied in the slave BF to generate an output. While this algorithm is in some ways attractive, it still requires enough target realizations to generate a good autocorrelation matrix; a requirement that cannot be met in medical ultrasound.

B. Widrow, K. M. Duvall, R. P. Gooch, and W. C. Newman, "Signal Cancellation Phenomena in Adaptive Antennas: Causes and Cures," *IEEE Trans. Antennas Propagat.*, vol. AP-30, no. 3, pp. 469-478, 1982.

REDUCED RANK BEAMFORMERS

The basic idea here is to save computation time by calculating a reduced rank autocorrelation matrix. All considerations made for the Capon BF still apply in this case. Principal Component (PC), and Multi-Stage Wiener Filter (MSWF) are example of such algorithms.

W. F. Gabriel, "Using Spectral Estimation Techniques in Adaptive Processing Antenna Systems," IEEE Trans. Antenna Propagat., vol. AP-34, no. 3, pp. 291-300, 1986.

S. M. Kogon, "Robust adaptive beamforming for passive sonar using eigenvector/beam association and excision," *Sensor Array and Multichannel Signal Processing Workshop Proceedings*, pp. 33-37, 2002.

J. S. Goldstein, I. S. Reed, and L. L. Scharf, "A Multistage Representation of the Wiener Filter Based on Orthogonal Projections," *IEEE Trans. Inform. Theory*, vol. 44, no. 7, pp. 2943-2959, 1998.

M. L. Honig and J. S. Goldstein, "Adaptive Reduced-Rank Interference Suppression Based on the Multistage Wiener Filter," *IEEE Trans. Commun.*, vol. 50, no. 6, pp. 986-994, 2002.

DETERMINISTIC BEAMFORMERS

The following beamformers do not make use of any statistics, therefore are suitable to use with only a single-snapshot of data. In general, this class of beamformer is much better suited to the problems we face in ultrasound imaging. These algorithms are relatively new and research is progressing rapidly in this domain.

ADAPTIVE SINGLE SNAPSHOT BEAMFORMER

This algorithm subdivides the array into G groups of K elements (the groups can overlap), and rearranges the data into a GxK matrix. For every steering direction, this beamforming scheme searches for the scalar α that reduced the rank of the data matrix. This scalar represents the magnitude of the signal coming from that particular look direction. This algorithm is based on the following observation: each source in the far field contribuites as 1 in the rank of the GxK matrix. In other words, if we assume L far field sources, the rank of the data matrix will be equal to L.

The ASS beamformer is designed for narrowband, far field signals. However, it can also be implemented in the frequency domain for broadband data. It is apparently not flexible enough to be applied to near-field signals however.

M. E. Ali and F. Schreib, "Adaptive Single Snapshot Beamforming: A New Concept for the Rejection of Nonstationary and Coherent Interferers," *IEEE Trans, Signal Processing*, vol. 40, no. 12, pp. 3055-3058, 1992.

DETERMINISTIC NULL STEERING (DNS)

The main idea behind this algorithm is to project the data into a sub-space that is orthogonal to the space spanned by the off-axis signals. In order to do that, the algorithms required knowledge of the DOAs of the signals that need to be null out. (If DOA's have to be estimated from the data, this algorithm should be considered a reduced rank adaptive BF).

In the narrowband case the algorithm is easily implemented, since the DOAs are one-dimensional steering vectors. However, in the broadband case, the computational complexity increases significantly since we have to deal with FIR filters (preferably matched filters) for every channel.

An advantage of this algorithm is that it requires no far-field assumption. Unfortunately algorithm performance is highly sensitive to mismatches in DOA. In simulations we concluded that this sensitivity was so great that this algorithm was unlikely to perform well with experimental ultrasound data.

H. Subbaram and K. Abend, "Interference Suppression Via Orthogonal Projections: A Performance Analysis," *IEEE Trans. Antennas and Propag.*, vol. 41, no. 9, pp. 1187-1194, 1993.

H. L. Van Trees, "Detection, Estimation, and Modulation Theory; Part IV: Optimum Array Processing," *John Wiley & Sons*, New York, 2002.

SOURCE LOCALIZATION ALGORITHMS

This class of algorithms takes a completely different approach. A signal model is first generated of the field produced by a series of hypothetical sources. Through some recursive algorithms, the sensors' output is matched to the signal model to solve for the position and intensity of the real sources. Statistics are not required and both near-field/far-field and broad/narrow band cases can be modeled (for the broadband case the system is usually modeled in the frequency domain).

The main problems with this class of algorithm are the high computational cost, the derivation of an accurate signal model, and possibly convergence. These limitations not withstanding, we have decided to focus our efforts on this class of algorithms.

R. Bethel, B. Shapo, and H. L. Van Trees, "Single Snapshot Spatial Processing: Optimized and Constrained," *Sensor Array and Multichannel Signal Processing Workshop Proceedings*, pp. 508-512, 2002.

D. M. Malioutov, M. Cetin, J. W. Fisher III, and A. S. Willsky, "Superresolution Source Localization Through Data-Adaptive Regularization," *Sensor Array and Multichannel Signal Processing Workshop Proceedings*, pp. 194-198, 2002.

After performing extensive literature searches and implementing and testing a number of the algorithms described above, we concluded that the algorithm described in "Single Snapshot Spatial Processing: Optimized and Constrained" offered the best possibility for success given the parameters of *in vivo* ultrasound imaging.

SPOC Progress:

Most of the Adaptive Beamforming algorithms previously described fail when applied to medical ultrasound data. This can be attributed to some or all of the following factors: we are operating in a near-field scenario, our signals are broadband, and we have limited statistical information available.

SPOC was first developed by Van Trees *et al.*. A similar approach has also been discussed by Malioutov *et al.*. This algorithm, briefly described below, can be successfully applied to medical ultrasound data.

The algorithm:

- The region of interest (ROI) is subdivided in a grid of hypothetical sources at arbitrary positions, as shown in figure 2. Finer grid sampling yields finer final resolution.
- For each point in the ROI, we calculate the hypothetical field received by the array for that specific point. These responses are included into the array manifold matrix **V** of dimensions LxP, where L and P are the numbers of hypothetical sources in the range and lateral dimensions, respectively.
- The data vector $\mathbf{x} = [x_1\ x_2\ \ldots\ x_N]$ is received by the N-element linear array. This vector can be modeled as $\mathbf{x} = \mathbf{V}*\mathbf{f}$. In this expression, **f** is the LPx1 signal vector, whose elements are the amplitudes of sources located in the ROI.
- Given **x** and **V**, SPOC recursively estimates the signal vector **f**.

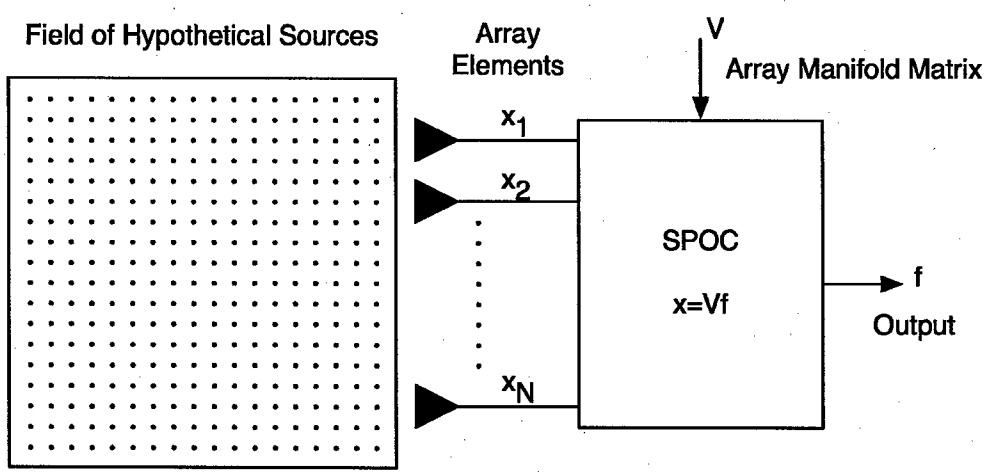

Figure 2. Schematic diagram of SPOC.

A series of computer simulations were performed in Matlab to test the potential of SPOC.

Point Target.

We simulated a 33 element linear array operating at 5 MHz with element spacing of 150 μm. A point target was placed in front of the transducer at a depth of 20.1 mm.

Hypothetical sources were placed every 20_m in range and every 100μm in azimuth.

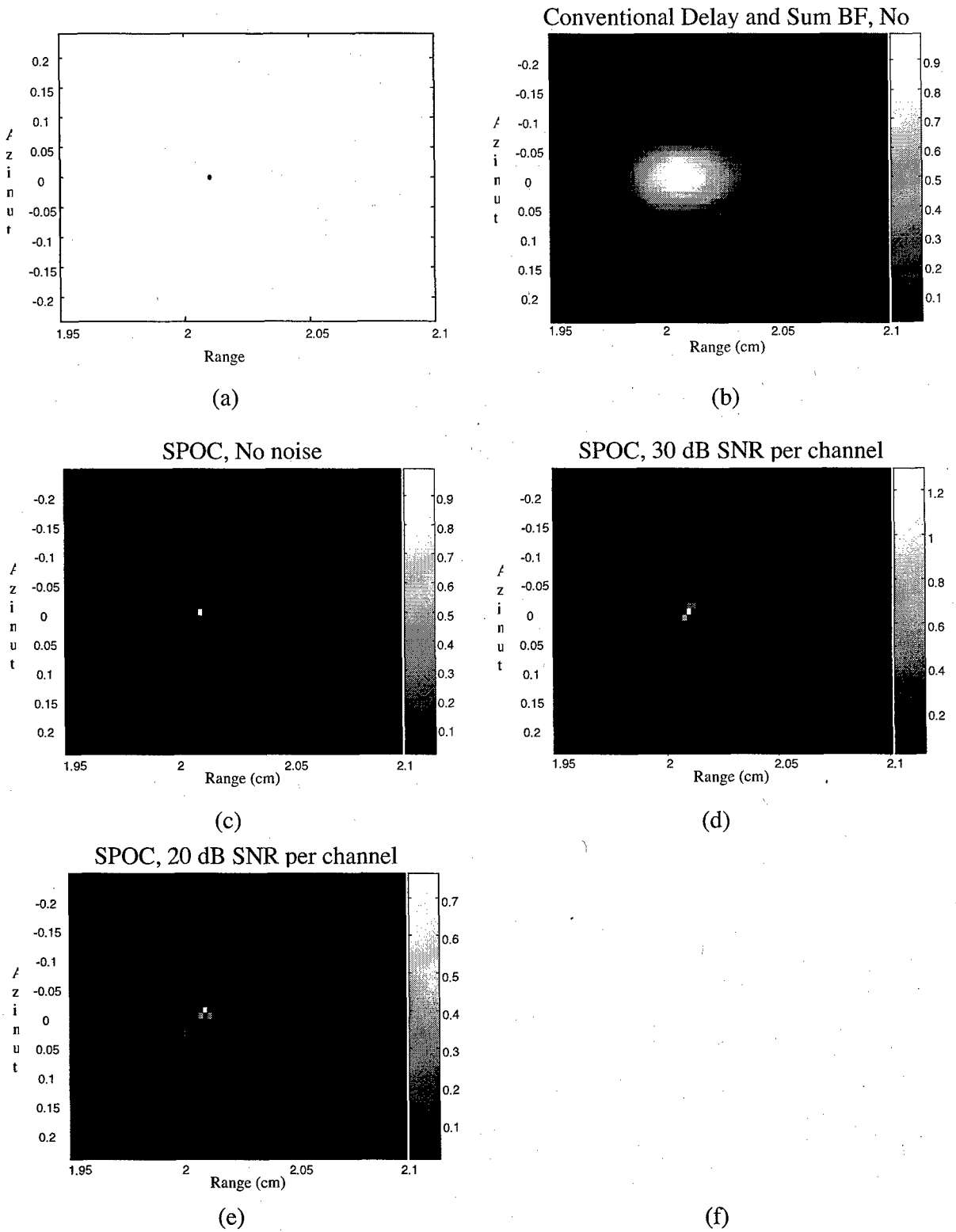

Figure 3. Results obtained simulating a point target. The point target is depicted in (a); (b) shows conventional delay-and-sum beamforming, whereas images (c) to (f) show SPOC with different levels of electronic noise.

Wire Targets.
We simulated a 33 element linear array operating at 5 MHz with element spacing of 150 μm. A series of wires were placed in front of the transducer at various depths and lateral positions.
Hypothetical sources were placed every 20μm in range and every 100μm in azimuth.

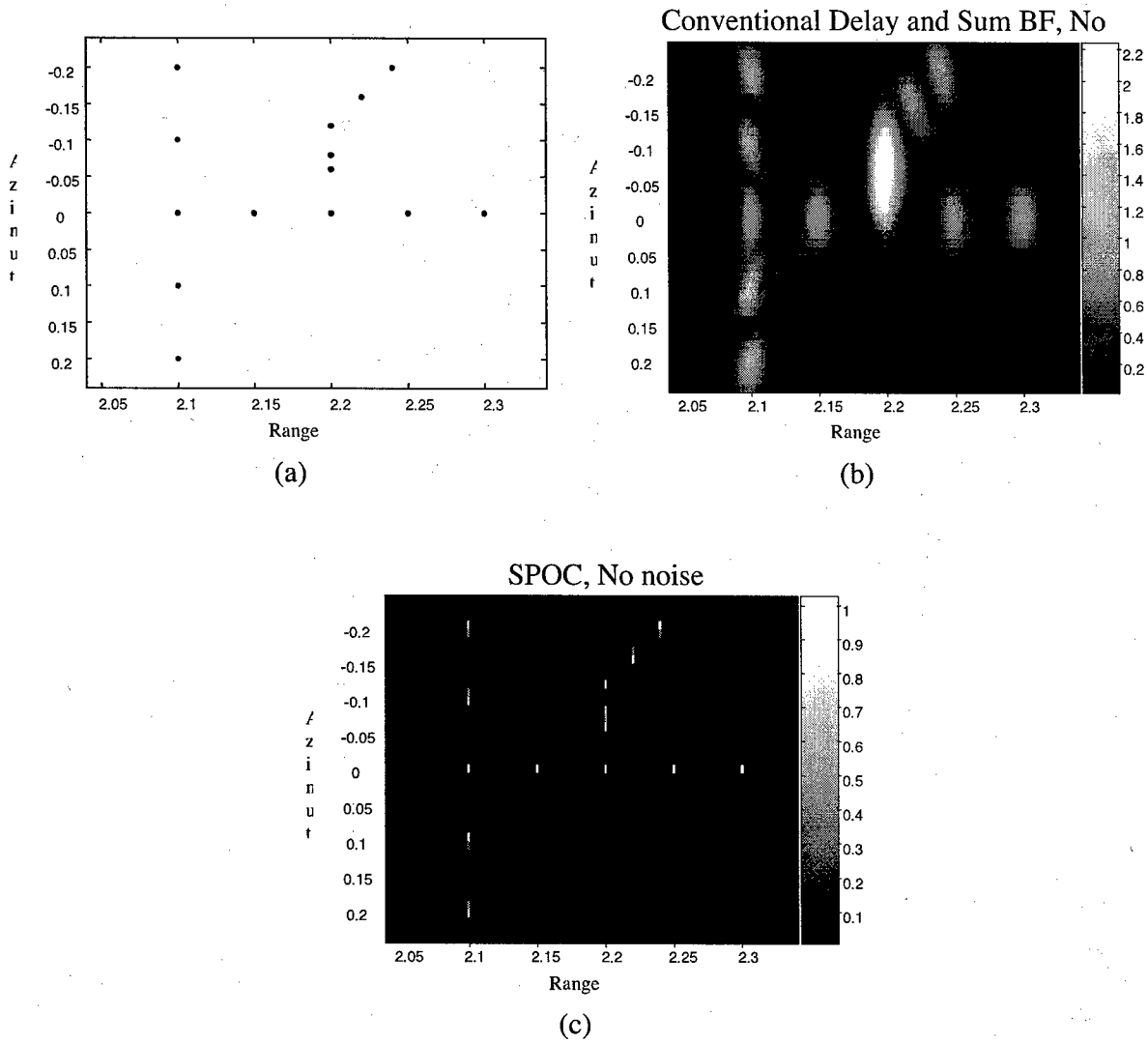

Figure 4. Results obtained simulating a series of wire targets. The wires are depicted in (a); (b) shows conventional delay-and-sum beamforming, whereas (c) show SPOC.

Anechoic Cyst.
We simulated a 33 element linear array operating at 5 MHz with element spacing of 150 μm. An anechoic cyst in a scattering environment was placed in front of the transducer.
Hypothetical sources were placed every 20μm in range and every 100μm in azimuth.

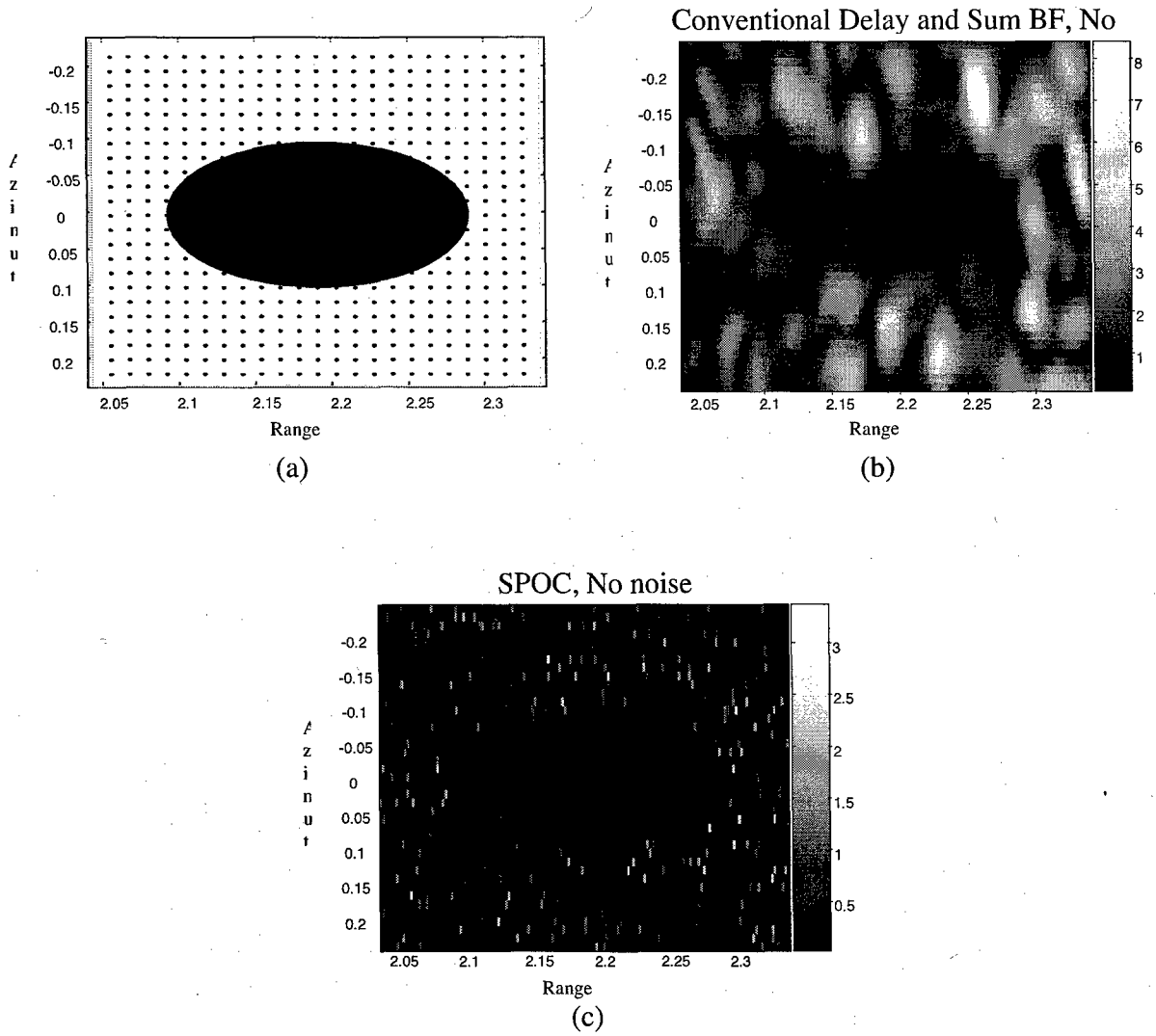

Figure 5. Results obtained simulating an anechoic cyst surrounded by scatterers. The cysts is depicted in (a); (b) shows conventional delay-and-sum beamforming, whereas (c) show SPOC.

Simulation Tool Development:
The performance of the SPOC algorithm depends greatly upon the quality of the system model it applies. In our initial simulations (presented above) we modeled the system using analytical methods, or using the well known FIELD program written by Jørgen Jensen. Unfortunately FIELD is quite slow when computing full 3D spatial impulse responses. Further, because FIELD works entirely on sampled data sets it is prone to artifacts from undersampling. We have implemented the Tupholme-Stepanishen method (the core approach used in FIELD) in a new piece of code we call DELFI. The DELFI code uses cubic spline representations of the transmitted pulse, and the transmit and receive spatial impulse responses. This approach avoids the potential sampling difficulties of FIELD. It is also significantly faster at computing space-space-space responses at an instant in time. These sort of responses are critical in much of our research and the 25 fold increase in speed for DELFI is of great significance. We have submitted a paper describing the algorithm and DELFI code [16]. Once this paper is

accepted for publication we will place the 1000 lines of DELFI source code on the Mathworks public access web site.

A limitation of the DELFI code is that it utilizes the same far-field approximation used by FIELD. This assumption requires intensive subsampling of the transducer array when the point of interest lies in the near-field of the transducer. We are currently refining the algorithm to be more accurate in the near-field. The modifications currently being explored would not have a significant impact on computational complexity. We anticipate completing and testing this refined algorithm in the coming year. We will submit a publication describing this work as it develops.

Experimental Platform Development:
Both the CAB algorithm described in our original proposal and the SPOC algorithm which we are now exploring require access to individual channel data within the ultrasound beamformer. Acquisition of such data, especially in real-time, is a daunting task. We are currently working with three different experimental platforms. Each of these has limitations, but together their capabilities are quite expansive.

Our first experimental system is a clinical GE Logiq 700 MR. This scanner acquires summed complex I/Q data under control of a set of custom pulse sequences and system tools. We are able to obtain single channel data by altering system apodization on successive transmissions. Acquisition of a complete single channel data set including transmit focusing is extremely slow with this method, however limited data sets can be acquired rapidly. In one strategy we translate a single transmit element and a single receive element across the array. This allows synthetic aperture (SA) focusing and CAB to be performed offline. Surprisingly this approach exhibits a single channel signal to noise ratio (SNR) of approximately 36 dB. Unfortunately tissue motion during acquisition can seriously degrade images formed using this method. We have recently implemented an alternate acquisition strategy which utilizes a focused transmit beam and a moving single element receive aperture to enable single channel acquisition. This approach will allow us to acquire a full set of single channel data for a few dozen image lines in the same period of time that would be required to acquire a normal frame of image data. While still somewhat slow, this approach should be less susceptible to tissue motion. We are currently testing this method.

Our second experimental system is a Philips SONOS 5500. This system also operates under custom control and acquires single channel data through system apodization. We are expanding upon this capability by modifying this system to acquire data in real-time and in parallel from all 128 beamformer channels. Once complete we will be able to acquire single channel data for up to 3.2 seconds. Note that single channel acquisition with this system will be in real-time and will include full use of transmit focusing. In the past year we have designed and tested the final circuit board needed for this system modification. Unfortunately testing revealed a fundamental flaw in that design. We have since redesigned the board and are now assembling it for test. We think it likely that this system will become functional in the first quarter of 2006.

A third experimental system, not described in the original proposal, is a fully custom system developed in a collaboration with two other investigators at the University of Virginia (John A. Hossack and Travis N. Blalock.) A second generation of this system is already being assembled. This second generation system will utilize a 3600 element 2D array and will operate at a 5.0 MHz center frequency. Data from all channels will be acquired in parallel in real-time, however only four real samples will be acquired by each channel. Although the data acquisition of this system is certainly limited in some ways, we believe that this system will provide an excellent testbed for SPOC. In the coming months as this system becomes operational we will acquire data to test the viability of SPOC on 2D arrays.

Key Research Accomplishments:

- Identification of a fundamental weakness of the CAB algorithm for ultrasound imaging

- Extensive review of adaptive beamforming literature
- MATLAB implementation and evaluation of a number of adaptive beamforming algorithms
- Identification of the SPOC adaptive beamforming algorithm

- MATLAB implementation of SPOC
- Extensive testing of SPOC for point targets and speckle generating targets
- Tested sensitivity of SPOC to electronic noise (not excessively sensitive)
- Tested sensitivity of SPOC to the effects of frequency dependent attenuation (some sensitivity, can be compensated for through modest algorithm adjustment)

- Conceived of and implemented the DELFI simulation tool
- Submitted a paper describing DELFI

- Identified problems with the SONOS experimental platform under development
- Revised design of the SONOS platform

- Submitted one patent disclosure on the use of SPOC in medical ultrasound
- Submitted multiple abstracts to scientific meetings describing the use of SPOC in medical ultrasound

Reportable Outcomes:

Papers:

Walker, W.F., "A Spline Based Approach for Computing Spatial Impulse Responses," submitted to IEEE Trans. Ultrason. Ferroelec. Freq. Contr., Feb., 2005.

Conference Abstracts:

Viola, F. and W.F. Walker, "Adaptive Signal Processing in Medical Ultrasound Beamforming," accepted to the 2005 IEEE Ultrasonics Symposium.

Viola, F., and W.F. Walker, "Adaptive Beamforming for Medical Ultrasound Imaging," U.S. Dept. of Defense Breast Cancer Research Program Era of Hope 2005 Meeting, June 2005.

Patent Disclosures:

"Adaptive Beamformiong for Medical Ultrasound Imaging," F. Viola, and W.F. Walker, patent disclosure filed 2005.

Software:

DELFI – A cubic spline based code for simulating spatial impulse responses. Currently over 1000 lines of C code.

Conclusions:

In our first year of funding we have identified a fatal flaw in the Constrained Adaptive Beamforming algorithm that was to be the core of our research effort in this grant. We have since explored the adaptive beamforming literature and identified an algorithm which is much better suited to our problem: Spatial Processing Optimized and Constrained. This algorithm is robust to noise and other common difficulties with ultrasound data. In the coming year we will test this algorithm on experimental data and obtain *in vivo* data allowing us to test the hypothesis that off axis scattering is a major source of image degradation in the breast.

References:

[1] V. Jackson, "Management of solid breast nodules: what is the role of sonography?," *Radiology*, vol. 196, pp. 14-15, 1995.

[2] V. P. Jackson, "The Role of US in Breast Imaging," *Radiology*, vol. 177, pp. 305 - 311, 1990.

[3] T. M. Kolb, J. Lichy, and J. H. Newhouse, "Comparison of the Performance of Screening Mammography, Physical Examination, and Breast US and Evaluation of Factors that Influence Them: An Analysis of 27,825 Patient Evaluations," *Radiology*, vol. 225, pp. 165-175, 2002.

[4] M. O'Donnell and S. W. Flax, "Phase aberration correction using signals from point reflectors and diffuse scatters: measurements," *IEEE Trans. Ultrason. Ferroelec. Freq. Contr.*, vol. 35, pp. 768-774, 1988.

[5] M. O'Donnell and S. W. Flax, "Phase aberration measurements in medical ultrasound: human studies," *Ultrasonic Imaging*, vol. 10, pp. 1-11, 1988.

[6] L. Nock, G. E. Trahey, and S. W. Smith, "Phase aberration correction in medical ultrasound using speckle brightness as a quality factor," *JASA*, vol. 85, pp. 1819-1833, 1989.

[7] S. Krishnan, P.-C. Li, and M. O'Donnell, "Adaptive Compensation of Phase and Magnitude Aberrations," *IEEE Transactions on Ultrasonics Ferroelectrics & Frequency Control*, vol. 43, pp. 44-55, 1996.

[8] L. M. Hinkelman, D.-L. Liu, R. C. Waag, Q. Zhu, and B. D. Steinberg, "Measurement and correction of ultrasonic pulse distortion produced by the human breast.," *Journal of the Acoustical Society of America*, vol. 97:3, pp. 1958-1969, 1995.

[9] G. Ng, P. D. Freiburger, W. F. Walker, and G. E. Trahey, "A technique for adaptive imaging in the presence of distributed aberrations," presented at IEEE Ultrasonics Symposium, Seattle, Washington, 1995.

[10] Q. Zhu and B. D. Steinberg, "Correction of multipath interference using clean and spatial location diversity," presented at IEEE International Ultrasonics Symposium, Seattle, Washington, 1995.

[11] K. Rigby, E. Andarawis, C. Chalek, B. Haider, W. Hinrichs, R. Hogel, W. Leue, M. Angle, B. McEathron, S. Miller, S. Peshman, M. Peters, L. Thomas, S. Krishnan, and M. O'Donnell, "Realtime Adaptive Imaging," presented at IEEE Ultrasonic Symposium, 1998.

[12] K. Rigby, C. Chalek, B. Haider, R. Lewandowski, M. O'Donnell, L. Smith, and D. Wildes, "Improved in vivo Abdominal Image Quality Using Real-Time Estimation and Correction of Wavefront Arrival Time Errors," presented at IEEE Ultrasonics Symposium, 2000.

[13] R. Gauss and G. Trahey, "Wavefront Estimation in the Human Breast," presented at SPIE Medical Imaging, 2001.

[14] J. A. Mann and W. F. Walker, "Constrained Adaptive Beamforming: Point and Contrast Resolution," presented at SPIE Medical Imaging Symposium, 2003.

[15] J. A. Mann and W. F. Walker, "A Constrained Adaptive Beamformer for Medical Ultrasound: Initial Results," presented at Proc. IEEE Ultrason. Symp., 2002.

[16] W. F. Walker, "A Spline Based Approach for Computing Spatial Impulse Responses," *IEEE Transactions on Ultrasonics Ferroelectrics & Frequency Control*, submitted.

Submitted as a CORRESPONDENCE to IEEE Trans. Ultrason. Ferroelec. & Freq. Contr.

A Spline Based Approach for Computing Spatial Impulse Responses

William F. Walker, Ph.D.
Department of Biomedical Engineering
Department of Electrical and Computer Engineering
University of Virginia
bwalker@virginia.edu

Abstract:

This paper describes an analytical approach for computing the two-way far-field spatial impulse response from rectangular transducer elements under arbitrary excitation. The described approach determines the response as the sum of polynomial functions, making computational implementation quite straightforward. The proposed algorithm was implemented as a C routine under Matlab and results were compared to theory and to those obtained under similar conditions from the well established FIELD II program. All results were in excellent agreement. The proposed method is quite efficient for computing spatial sensitivity functions at a single instant in time; an application for which FIELD II is not well optimized. Under the specific conditions tested here, the proposed algorithm was approximately 25 times faster than FIELD II for computing spatial sensitivity functions, with no loss in quality.

Introduction:

The design of modern phased array ultrasonic imaging systems relies heavily on the use of computer simulations. This is necessary because the broadband and near-field nature of most clinical imaging environments severely limits the utility of the Fraunhofer approximation [1] and other theoretical methods. Furthermore, the high degree of optimization of modern systems makes even small deviations from theory significant. For example, if the system designer is concerned with the array sensitivity pattern down 80 dB from the main-lobe, then a deviation from theory of only 0.1% (-60dB) will significantly affect performance and make optimization to the desired level impossible. Clearly, highly accurate simulation tools are required to guide the selection of transducer geometry, apodization, operating frequency, and other parameters.

While most researchers and designers would agree upon the need for accurate simulation, the appropriate approach depends upon the specific problem of interest and the parameters that are most significant to that problem. For example, in cases where details of transducer vibration and crosstalk are of interest, a computationally costly finite element analysis may be required to capture the most relevant behavior. For such problems the highly optimized PZFlex (Weidlinger Associates, Inc. New York, NY) package is widely used [2]. In other cases, where the detailed transducer response is of less interest, but the propagation medium is inhomogeneous or multiple scattering occurs, the more computationally efficient Finite Difference Method, such as that implemented in Wave2000 (CyberLogic Inc., New York, NY), may be used.

For the vast majority of situations, where the propagation medium can be considered homogeneous or inhomogeneities can be modeled as a near-field thin phase

screen, Stepanishen's method [3], as implemented in Jørgen Jensen's FIELD II program [4] has become a *de facto* standard. This approach determines the spatial impulse response of each transmit element, convolves this with the spatial impulse response of each receive element, convolves this result with the transmitted pulse, and convolves this with the transmit and receive electromechanical impulse responses to determine the two-way temporal response at a point in space. This technique, as implemented in Jensen's code, has been highly refined over roughly a decade of development so that it is extremely efficient and available in a compiled form on a variety of computer platforms (http://www.es.oersted.dtu.dk/staff/jaj/field/). By computing the temporal signals returned from various target locations, FIELD II readily models common experimental situations.

While the temporal response returned by FIELD II provides an excellent parallel to experiment, recent theoretical work by Zemp [5] and Walker [6] highlights the importance of considering the full four or five dimensional system response. In a previous paper [6], this author discussed a general signal model describing the system response as a function of three spatial dimensions and time. While much of this detail is hidden experimentally, the consideration of the full dimensionality of the system response yields insights and offers paths for analysis that are not apparent in the more conventional two dimensional (space, time) view of the system. Zemp [5] carried this concept one step further, including another dimension for image line index, thereby further clarifying system behavior. Our laboratory has recently applied these frameworks to derive a general resolution metric that allows quantitative comparison of system performance, even when the individual impulse responses of those systems are very different in structure [7]. Interestingly, this new resolution metric is based upon the system response throughout space at a single instant in time; a form of the impulse response that is not naturally determined by FIELD II. Although such responses can be computed by sampling the temporal responses generated by FIELD II, this approach is extremely costly in terms of both computation and storage.

In this paper we describe a new approach to computing spatial impulse responses that directly determines the response throughout space at a single instant in time. This approach is complementary to FIELD II, simply yielding responses in a different set of dimensions. Because results from this code are predictive of system performance and are a permutation of the data available from FIELD II, we name this code DELFI. In this paper we describe the theoretical underpinnings of the DELFI code, describe implementation, and validate the code through comparisons with FIELD II and analytical predictions. We discuss the relative computational efficiency of DELFI and discuss future directions for development and refinement.

Theory:

We begin our derivation by considering the general approach employed by Jensen in the FIELD II program [4]. We consider the system response for a specific transmit-receive element pair to be a four dimensional function of space and time:

$$p(x,y,z,t) = e(t) \underset{t}{*} m_t(t) \underset{t}{*} m_r(t) \underset{t}{*} h_t(x,y,z,t) \underset{t}{*} h_r(x,y,z,t) \qquad (1)$$

where x, y, and z are the three spatial dimensions, t is the time for a given line (proportional to range in the beamformed image), $p(x,y,z,t)$ is the system point spread function (psf), $e(t)$ is the electrical excitation of the transmit element, $m_t(t)$ and $m_r(t)$ are the electromechanical transfer functions of the transmit and receive elements respectively, $h_t(x,y,z,t)$ and $h_r(x,y,z,t)$ are the spatial impulse responses of the transmit and receive elements respectively, and $\underset{t}{*}$ indicates convolution in the time dimension. In typical systems the excitation and the transmit and receive electromechanical transfer functions are assumed constant for all elements of the array. Thus we can convolve these terms together before computing the overall response with little loss in generality. Performing this step we simplify (1) to yield:

$$p(x,y,z,t) = emm_{tr}(t) \underset{t}{*} h_t(x,y,z,t) \underset{t}{*} h_r(x,y,z,t) \tag{2}$$

where $emm_{tr}(t)$ is the combined effect of the excitation and the transmit and receive electromechanical transfer functions and can be represented mathematically as $emm_{tr}(t) = e(t) \underset{t}{*} m_t(t) \underset{t}{*} m_r(t)$. While FIELD II computes expressions (1) or (2) using sampled versions of each of the component signals, we take an alternate approach, instead using analytical expressions for these functions.

The utility of an analytical approach depends upon the choice of expressions used: they must be general enough to include all relevant cases, but they must be constrained in such a way to guarantee the presence of an analytical solution. Since (2) allows for consideration of most practically interesting cases and requires two convolutions (rather than the four convolutions of (1)) we build our algorithm upon this expression. Further simplification can be made by assuming that the point of interest lies in the far-field of both the transmit and receive elements. This is not an onerous assumption since cases where the response would lie in the near-field of a physical element can be readily modeled using a superposition of computational elements for which the far-field assumption is valid. We further simplify the problem by assuming that the elements are rectangular.

Following these assumptions, and once again drawing upon the methodology of Jensen [4], we recognize that the one-way spatial impulse response of an element takes on one of three functions. If the field point lies on a line perpendicular to the element face and passing through its center then the spatial impulse response as a function of time is simply a delta function, as shown in the left panel of figure 1. If the field point does not fulfill the first condition, but instead lies upon one of two planes passing through the element center and perpendicular to the element edges then the spatial impulse response in time is a rectangle function, as depicted in the central panel of figure 1. Finally, if the field point fulfills neither of the above conditions then the spatial impulse response in time is a trapezoid function, as shown in the right panel of figure 1. These possible one-way spatial impulse responses are summarized mathematically below. Note we describe the rectangle and trapezoid functions using sums of unit step and ramp functions.

$$h_0(x,y,z,t) = A_0(x,y,z)\delta(t - t_0) \tag{3}$$

$$h_1(x,y,z,t) = A_1(x,y,z)u(t-t_{1,0}) - A_1(x,y,z)u(t-t_{1,1}) \tag{4}$$

$$\begin{aligned} h_2(x,y,z,t) = {} & (t-t_{2,0})A_2(x,y,z)u(t-t_{2,0}) - (t-t_{2,1})A_2(x,y,z)u(t-t_{2,1}) \\ & -(t-t_{2,2})A_2(x,y,z)u(t-t_{2,2}) + (t-t_{2,3})A_2(x,y,z)u(t-t_{2,3}) \end{aligned} \tag{5}$$

where h_0, h_1, and h_2 represent the delta, rectangle, and trapezoid spatial impulse responses respectively and $u(t)$ is the unit step function. The scaling functions $A_0(x,y,z)$, $A_1(x,y,z)$, and $A_2(x,y,z)$ are constant at any specific spatial location and include $1/r$ spreading, scaling to account for the element size, and an obliquity factor to account for a soft transducer baffle [8], if desired. The time delay t_0 present in (3) is determined by the speed of sound and the distance from the element center to the field point. Similarly, the delays present in (4) and (5) are determined from the speed of sound and distances between the field point and the element edges and corners, respectively.

To determine the two-way response from an element pair we must convolve the appropriate version of (3)-(5) for the receive element with the appropriate version of (3)-(5) for the transmit element. While superficial analysis suggests that nine permutations are possible, a more careful examination reveals that since the order of convolution is irrelevant, some of these permutations are redundant. Thus, the two-way response must fit one of the following six general expressions.

$$h_{tr} = h_t \underset{t}{*} h_r = \left\{ h_0 \underset{t}{*} h_0 \text{ or } h_0 \underset{t}{*} h_1 \text{ or } h_0 \underset{t}{*} h_2 \text{ or } h_1 \underset{t}{*} h_1 \text{ or } h_1 \underset{t}{*} h_2 \text{ or } h_2 \underset{t}{*} h_2 \right. \tag{6}$$

where we have dropped space and time references to simplify notation. Note that while the simplified notation of (6) suggests that in some cases (such as $h_0 \underset{t}{*} h_0$) the transmit and receive responses are identical, this is intended only to state that the transmit and receive responses fit the same function; they may have different delays and scaling. Substituting (3)-(5) into (6) yields a set of six possible two-way impulse responses:

$$h_{0_a} \underset{t}{*} h_{0_b} = A_{0_a} A_{0_b} \delta(t - t_{0_a} - t_{0_b}) \tag{7}$$

$$h_0 \underset{t}{*} h_1 = A_0 A_1 \sum_{j=0}^{1} (-1)^j u(t - t_0 - t_{1,j}) \tag{8}$$

$$h_0 \underset{t}{*} h_2 = A_0 A_2 \sum_{j=0}^{3} c_j (t - t_0 - t_{2,j}) u(t - t_0 - t_{2,j}) \tag{9}$$

$$h_{1_a} \underset{t}{*} h_{1_b} = A_{1_a} A_{1_b} \sum_{j=0}^{1} \sum_{k=0}^{1} (-1)^j (-1)^k (t - t_{1_a,j} - t_{1_b,k}) u(t - t_{1_a,j} - t_{1_b,k}) \tag{10}$$

$$h_1 \underset{t}{*} h_2 = A_1 A_2 \sum_{j=0}^{1} \sum_{k=0}^{3} (-1)^j c_k \left(t - t_{1,j} - t_{2,k}\right)^2 u\left(t - t_{1,j} - t_{2,k}\right) \tag{11}$$

$$h_{2_a} \underset{t}{*} h_{2_b} = A_{2_a} A_{2_b} \sum_{j=0}^{3} \sum_{k=0}^{3} c_j c_k \left(t - t_{2_a,j} - t_{2_b,k}\right)^3 u\left(t - t_{2_a,j} - t_{2_b,k}\right) \tag{12}$$

where $c_j = \{1 \; for \; j = 0 \; or \; 3 \quad and \quad -1 \; for \; j = 1 \; or \; 2\}$. With each of the six possible two-way impulse responses in hand we can now consider an appropriate analytical representation of the excitation function (including transmit and receive electromagnetic transfer functions). While a number of possible functions are attractive, we choose to represent $emm_{tr}(t)$ using cubic splines [9]. This representation is attractive because it allows arbitrary function shapes while restricting the form of the function to be no higher order than piecewise cubic polynomial. Writing this spline representation explicitly yields:

$$emm_{tr}(t) = \sum_{j=M_0}^{M_1} \left(\alpha_j + \beta_j t + \gamma_j t^2 + \delta_j t^3\right)\left(u(t - j\partial) - u\left(t - (j+1)\partial\right)\right) \tag{13}$$

where α_j, β_j, γ_j, and δ_j are the spline coefficients, M_0 and M_1 are the first and last spline indices, and ∂_j is the spline to spline interval. We can now complete an analytical expression for (2) by convolving (13) with the appropriate version of (7)-(12). While such a convolution appears quite tedious, it can be readily performed utilizing Laplace transforms [10]. The resulting expression is a sum of 3rd, 4th, 5th, 6th, or 7th order polynomials (multiplied by unit step functions), with the polynomial order depending upon the combination of element responses employed. We do not present the analytical form of these expressions since they offer little insight and are quite lengthy. Utilizing these final polynomial expressions, the complete two-way response for a given transmit-receive element pair can be computed by simply summing polynomials.

Validation:

The proposed algorithm was implemented in a C routine called as a mex file within Matlab (The Mathworks, Inc. Natick, MA). This approach allowed us to readily generate array geometries and visualize results within Matlab, while taking advantage of the increased computational efficiency of compiled C. All calculations were performed in IEEE Standard double precision floating point arithmetic. All simulations were performed on an Apple Powerbook G4 computer running Matlab 7.0.1 under Mac OS 10.3.7.

The validity of the proposed algorithm was tested by comparing the two-way spatial response of a single 2D array element as predicted by DELFI and FIELD II. For both codes the array element was modeled using a single computational element. Both codes also assumed a combined excitation and transmit/receive electromechanical impulse response equal to a 5.0 MHz sine multiplied by an 8 cycle Nuttall window [11]. The spline representation of the pulse utilized in DELFI was generated at a sampling rate

of 8 times the assumed center frequency (40 MHz). This sampling rate was found empirically to generate a pulse with harmonics approximately 100 dB down from the main signal. FIELD II calculations utilized a sampling rate 5 times higher than this (200 MHz). While this rate is twice the default for FIELD II (100 MHz), our experience suggests that this rate is certainly within an appropriate range for calculations of this type. The system response was determined in radial coordinates over an angle of 0° to 90° (sampled at 0.45°) covering a range from 19.925 cm to 20.075 cm (sampled at 10 μm). For DELFI all points were computed at the time instant that centered the sensitivity function at 20 cm. For FIELD II a complete response in range, azimuth, and time was computed, with the time that centered the sensitivity function at 20 cm selected for analysis.

Typical DELFI and FIELD II sensitivity functions for a 300 x 300 μm element are shown in figure 2. Both responses have been normalized to allow comparison. These responses are quite similar except for a series of artifacts located about the 0° line in the FIELD II response. Although the source of this artifact is not apparent, it may result from the corrections FIELD II employs when sampling the infinite bandwidth spatial impulse responses of the array elements.

Additional simulations were performed to determine computational times and the similarity of responses for square elements ranging in size from 50 to 600 microns. All computational times were estimated using the tic and toc commands in Matlab. Across this set of 12 simulations the computation time for DELFI ranged from approximately 0.21 to 0.29 seconds. Over the same set of conditions FIELD II execution times ranged from 5.33 to 7.61 seconds. Comparing matched sets of simulations, FIELD II took from 18.4 to 33.6 times as long for the computation, with the average time of computation being 27.1 times greater for FIELD II. Note that these times do not include any array definitions or other housekeeping operations. For the sake of comparison we also computed the temporal response at the focus using both codes. FIELD II computations were performed at a sampling rate of 200 MHz and the DELFI code was run repeatedly at different time points to generate a waveform sampled at 40 MHz. Under these conditions the FIELD II response was computed in 1.2 ms and the DELFI response was computed in 7.2 ms, giving FIELD II a factor of 6 advantage in computational time. This difference is surprisingly modest given that DELFI was called 65 times from within a loop in Matlab, a process that engendered significant overhead. Straightforward modifications of DELFI might significantly improve its relative performance when temporal responses are required. While it would be inappropriate to over-generalize from this limited set of simulations, the existing DELFI code is computationally attractive for applications where spatial responses at a single time point are desired.

The accuracy of DELFI was quantified by computing the Full Width at Half Maximum (FWHM) of the two-way single element sensitivity function over a range of element sizes ranging from 50 to 600 microns in 50 micron steps. The same metric was also computed for FIELD II simulations, with both results compared to the iterative theoretical method of [12]. McKeighen's iterative method determines the element's FWHM sensitivity by modeling the response as a sinc squared multiplied by a cosine squared obliquity term (to account for an assumed soft baffle condition). McKeighen's method was implemented using 100 iterations at an assumed center frequency of 5.0 MHz. FIELD II and DELFI used sampling rates and the pulse definitions described

above. The FWHM of the spatial sensitivity function was estimated from the curve formed by taking the maximum of each lateral line, after computing the absolute value of the response. Results comparing FIELD II, DELFI, and McKeighen's theory are shown in figure 3. All three methods are in excellent agreement.

Discussion:

Computing the spatial impulse response of a transmit-receive element pair by convolving (13) with (7)-(12) analytically offers both advantages and disadvantages relative to the established approach using discrete time convolution. On the positive side the analytical approach allows direct computation of the response at a single instant in time. In contrast, the conventional discrete time approach (at least as currently implemented) requires the computation of a full temporal response even if only a single time point is required. An additional advantage of the analytical approach is that it yields an exact solution, at least within the numerical precision of the computer used for the calculation and within the limitations of the far-field approximation. In contrast, the discrete time approach utilizes under-sampled versions of the element responses and thus introduces some error. In addition, the discrete implementation makes it difficult to compute the spatial response at any exact instant in time. A relative weakness of the analytical approach is that significantly more computation is required to determine a temporal response at a single location. A further limitation of the analytical approach, at least as implemented here, is the occasional numerical instability that results from subtracting multiple high-order polynomials.

The DELFI code described here is still in an early stage of development, with many directions apparent for enhancing computational efficiency and improving accuracy. The current code determines the result of the convolution of a single spline segment with two trapezoid functions by summing 16 7th order polynomials. This approach is computationally tedious and prone to numerical instability. One possible direction for simplification would begin with the recognition that the first half of this response (in time) requires only 8 polynomials for synthesis. Next, by considering the response in negative time it is apparent that the second half (again in time) of this response also requires only 8 polynomials. Together this realization could cut computation time in half. Additional computational savings are undoubtedly possible. Algorithmic accuracy could be enhanced by utilizing a more sophisticated model for the element impulse responses. Spline functions might prove particularly suitable for modeling complicated near-field responses [13, 14].

Conclusion:

The DELFI code presented here employs analytical convolution of cubic spline functions with continuous time element responses to compute the spatial impulse response of ultrasound transducers. Comparison with FIELD II and theoretical methods show that the proposed algorithm performs comparably to existing methods. For the computation of impulse responses at a single instant in time, the proposed algorithm is as much as 30 times faster than FIELD II. For computing temporal responses the proposed code is approximately 6 times slower than FIELD II, although further refinement may reduce this mismatch. The proposed algorithm, as implemented by the DELFI code, offers an attractive complement to the well established FIELD II program.

Submitted as a CORRESPONDENCE to IEEE Trans. Ultrason. Ferroelec. & Freq. Contr.

Acknowledgements:

This work was supported in part by NIH Grant EB002348 and the US Army Congressionally Directed Research Program under Grant DAMD17-01-1-0443. The author would like to thank Drake Guenther and Karthik Ranganathan for their valuable feedback on this manuscript.

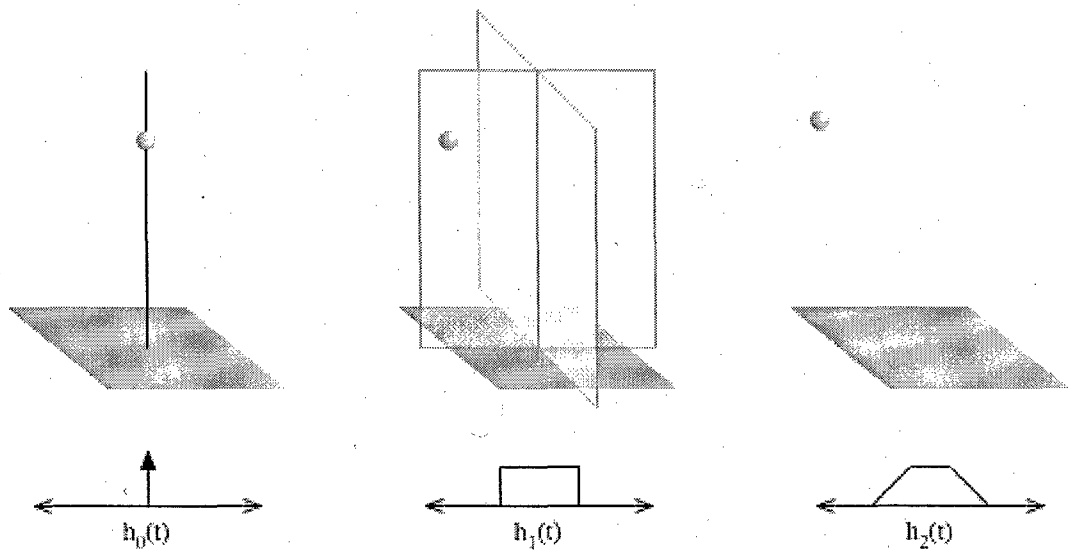

Figure 1:
Geometries for determining the one-way spatial impulse response of an individual array element. In the left panel the field point lies on a line through the element's center and perpendicular to its face. In the center panel the field point does not satisfy the first condition, but lies on a plane that bisects the element and is perpendicular to its face. In the right panel the field point lies at any location not satisfying either of the first two conditions.

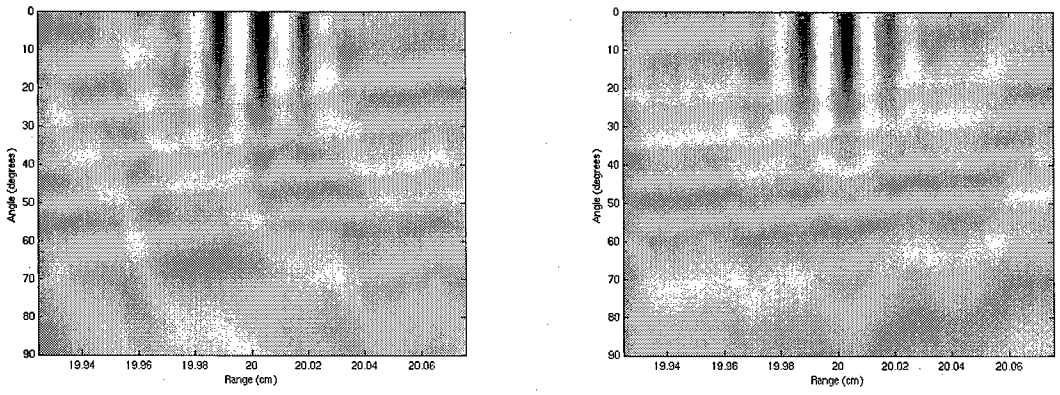

Figure 2:
The spatial impulse response of a 300 μm square array element in a soft baffle for an 8 cycle Nuttall windowed 5.0 MHz transmit pulse. The left panel depicts the output of the proposed algorithm (DELFI) while the right panel indicates the output of FIELD II. Both responses have been normalized to allow easy comparison. The responses are nearly identical with the exception of localized artifacts near the 0° line of the FIELD II response.

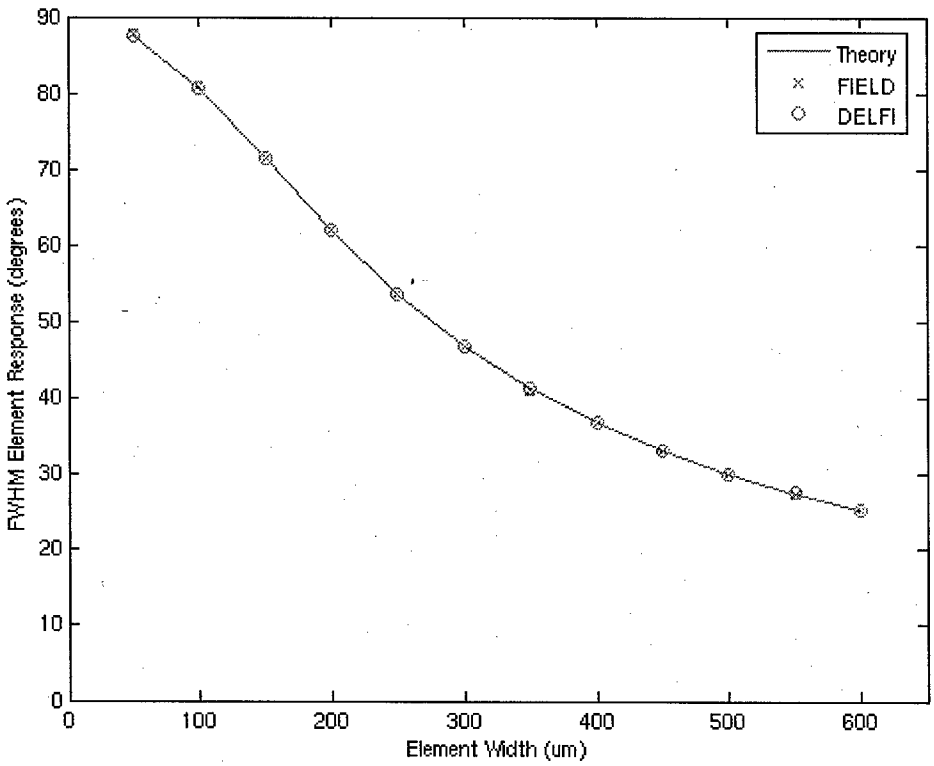

Figure 3:
Full Width at Half Maximum of the spatial sensitivity function of a square 2D array element. All analyses / simulations were performed at a 5.0 MHz center frequency with the soft baffle assumption. All methods are clearly in excellent agreement.

References:

[1] J. W. Goodman, *Introduction to Fourier Optics*. San Francisco: McGraw-Hill, 1986.

[2] G. L. Wojcik, D. K. Vaughan, N. Abboud, and J. Mould, "Electromechanical modeling using explicit time-domain finite elements," presented at Proc. 1993 Ultrasonics Symposium, Baltimore, 1993.

[3] P. R. Stepanishen, "Transient Radiation from Pistons in an Infinite Baffle," *Journal of the Acoustical Society of America*, vol. 49, pp. 1629-1638, 1970.

[4] J. A. Jensen and N. B. Svendsen, "Calculation of pressure fields from arbitrarily shaped, apodized, and excited ultrasound transducers," *IEEE Transactions on Ultrasonics, Ferroelectrics, and Frequency Control*, vol. 39, pp. 262-267, 1992.

[5] R. J. Zemp, C. K. Abbey, and M. F. Insana, "Linear system models for ultrasonic imaging: application to signal statistics," *IEEE Transactions on Ultrasonics Ferroelectrics & Frequency Control*, vol. 50, pp. 642-54, 2003.

[6] W. F. Walker, "The Significance of Correlation in Ultrasound Signal Processing," presented at SPIE International Symposium on Medical Imaging, San Diego, CA, 2001.

[7] K. Ranganathan and W. F. Walker, "A New Performance Analysis Metric for Medical Ultrasound," presented at IEEE Ultrasonics Symposium, Montreal, Canada, 2004.

[8] A. R. Selfridge, G. S. Kino, and B. T. Khuri-Yahub, "A theory for the radiation pattern of a narrow strip acoustic transducer," *Applied Physics Letters*, vol. 37, pp. 35-6, 1980.

[9] C. de Boor, *A Practical Guide to Splines*: Springer-Verlag, 1978.

[10] S. Haykin and B. Van Veen, *Signals and Systems*, 2 ed: Wiley, 2003.

[11] A. H. Nuttall, "Some Windows with Very Good Sidelobe Behavior," *IEEE Transactions on Acoustics, Speech, and Signal Processing*, vol. ASSP-29, pp. 84-91, 1981.

[12] R. E. McKeighen, "Design Guidelines for Medical Ultrasonic Arrays," presented at SPIE Medical Imaging: Ultrasonic Transducer Engineering, San Diego, CA, 1998.

[13] J. A. Hossack and G. Hayward, "Efficient calculation of the acoustic radiation from transiently excited uniform and apodised rectangular apertures," presented at IEEE Ultrasonics Symposium, 1993.

[14] J. A. Jensen, "A New Calculation Procedure for Spatial Impulse Responses in Ultrasound," *Journal of the Acoustical Society of America*, vol. 105, pp. 3266-74, 1999.